HiSST: International Conference on
High-Speed Vehicle Science Technology
26–29 November 2018, Moscow, Russia

Ultra-fast Temperature Sensitive Paint Shock Tunnel Heat Flux Measurements on the Intake of the LAPCAT II Small Scale Flight Experiment Configuration

Jan Martinez Schramm[1], Sebastian Karl[2], Klaus Hannemann[3] and Hiroshi Ozawa[4]

Abstract

A small scale flight experiment (SSFE) configuration powered by a Mach 8 scramjet was designed within the European Commission co-funded project Long Term Advanced Propulsion Concepts and Technologies (LAPCAT) II. The main objective of the test campaigns conducted in the High Enthalpy Shock Tunnel Göttingen (HEG) of the German Aerospace Center was to demonstrate that the numerically predicted positive aero-propulsive balance of the SSFE could be confirmed experimentally. The experiments were performed for a flight condition of Mach 7.4 at 27 km altitude. The positive aero-propulsive balance could be demonstrated utilizing the free flight force measurement technique based on optical tracking. Additionally, pressure and heat flux measurements were conducted on the intake, in the combustion chamber and on the thrust nozzle. Subsequent comparison to numerical predictions led to the conclusion, that one reason for the observed discrepancies could be the state of the hypersonic boundary layer on the intake. For the design, a fully turbulent boundary layer was assumed since no direct evidence of the real behavior was available. Therefore, the laminar to turbulent boundary layer transition process on the intake was studied in the framework of the development of an ultra-fast temperature sensitive paint (TSP) technique in HEG. The necessary prerequisites, which have to be fulfilled to apply TSP in a free piston driven shock tunnel, and the experimental setup for the scramjet intake measurements as well as the data evaluation procedure with special focus on the accuracy of the TSP technique, are discussed. The complex boundary layer transition process on the intake is characterized and the transition line is determined based on a combined experimental and numerical evaluation procedure. Further, information on the transition behavior extracted from this analysis is used as input for a numerical study using a Reynolds stress based turbulence model. The difference between the design assumption of a fully turbulent boundary layer and the transitional case is highlighted.

Keywords: Scramjet, intake flow, laminar turbulent boundary layer transition, shock tunnel testing, Temperature Sensitive Paint (TSP), CFD

Nomenclature

q_s	- surface heat flux
l	- length
l_B	- thickness of base layer
l_{TSP}	- thickness of TSP layer
T	- temperature
t	- time
n	- number of images/frames/measurements
λ	- wavelength
λ_{ex}	- excitation wavelength
λ_{em}	- emission wavelength
λ_{self}	- self-illumination
p	- pressure
ρ	- density

[1] *Group Leader Aerothermodynamics, DLR, Bunsenstraße 10, 37073 Göttingen, Jan.Martinez@dlr.de*
[2] *Group Leader Numerical Aerothermodynamics, DLR, Bunsenstraße 10, 37073 Göttingen, Sebastian.Karl@dlr.de*
[3] *Head Spacecraft Department, DLR, Bunsenstraße 10, 37073 Göttingen, Klaus.Hannemann@dlr.de*
[4] *Assistant Professor, Tokyo Metropolitan University (TMU), Asahigaoka 6-6, Hino, Tokyo, hozawa@tmu.ac.jp*

1. Introduction

The accurate quantification of the surface heat flux on the intake of a scramjet engine and the derived transitional boundary layer behavior is crucial for the proper operation as well as numerical simulation of the complete engine. Although computational fluid dynamics (CFD) can support to acquire a more and more in depth knowledge of the flow past complex configurations, the difficulty in accurately modeling the boundary-layer transition process remains and shows among other reasons the need for dedicated experiments. For surface heat flux measurements in shock tunnels, traditionally, surface-mounted temperature sensors, such as thermocouples and thin film gauges, have been widely used during the last decades (see, e.g., Schultz and Jones [1]). These sensors have response times of microseconds, and thus data can be sampled with high time resolution; however, the spatial resolution is less satisfactory. The packing density is limited by the sensor size and it is difficult to mount sensors on narrow and curved geometries. The installation of a large numbers of transducers results in complicated wiring and high cost. The clear advantages of temperature sensitive paint (TSP) over the classical techniques are the non-intrusive measurement approach and high spatial resolution. Image-based temperature measurements using TSP are accomplished by coating the model surface with paint and illuminating the surface with light of appropriate wavelength. This excitation process will force the luminophore in the TSP to emit light at a different wavelength. The luminescence from the paint is detected through a bandwidth-pass filter to separate the luminescence from the excitation light. It is a function of the local spatial temperature, and, therefore, each pixel on the camera acts as a thermocouple. In order to apply the technique in facilities such as the High Enthalpy Shock Tunnel Göttingen (HEG), with test times in the order of a few milliseconds, it is not only necessary to perform extensive calibration of the technique, but it is also required to fulfill specific requirements to obtain accurate heat flux distributions.

In the present study, TSP is applied to determine the laminar to turbulent boundary layer transition process on the intake of the scramjet driven small scale flight experiment (SSFE) configuration which was designed in the framework of the European Commission co-funded project LAPCAT II project [2]. Subsequently the data is used as input for the numerical modelling of the transitional intake flow.

2. High Enthalpy Shock Tunnel Göttingen, HEG

The High Enthalpy Shock Tunnel Göttingen (HEG) of the German Aerospace Center, DLR, is one of the major European hypersonic test facilities. This free piston driven shock tunnel [3,4,5] was commissioned for use in 1991 and has been utilized extensively since then in a large number of national and international space and hypersonic flight projects. The free piston driver concept is proposed by Stalker [6] and, therefore, the tunnels are also referred to as Stalker tubes. Originally, HEG was designed for the investigation of the influence of high temperature effects such as chemical and thermal relaxation on the aerothermodynamics of entry or re-entry space vehicles. Hardware extensions of the HEG allowed to extend the tunnel's operating range and included the establishment of a number of low total specific enthalpy conditions for integrated scramjet engine ground-based testing. In free piston driven shock tunnels, the conventional driver is replaced by a free piston driver as proposed by Stalker (see Fig 1). This type of facility consists of a secondary reservoir, a compression tube, separated from an adjoining shock tube via the primary diaphragm, and a subsequent nozzle, test section and dump tank. The overall length of HEG is 62 m and it weighs 280 t; approximately one third of its weight is contributed by an inert mass which is used to reduce the tunnel recoil motion. The compression tube is closed and sealed by a hydraulic oil system at the main diaphragm station. The shock tube is connected to the nozzle of the tunnel at the downstream closure, which is also driven by oil hydraulics to close and seal the tunnel. The compression tube has a length of 33 m and a diameter of 0.55 m. The shock tube is 17 m long with a diameter of 0.15 m. The HEG was designed to provide a pulse of gas to a hypersonic convergent-divergent nozzle at stagnation pressures of up to 200 MPa, and stagnation enthalpies of up to 23 MJ/kg. Regarding the test gas, no basic limitations exist. The operating condition used in HEG to perform the present

experiments is related to the test gas air and HEG operating condition XIII is used. In Table 1, the nominal reservoir and free stream condition is given.

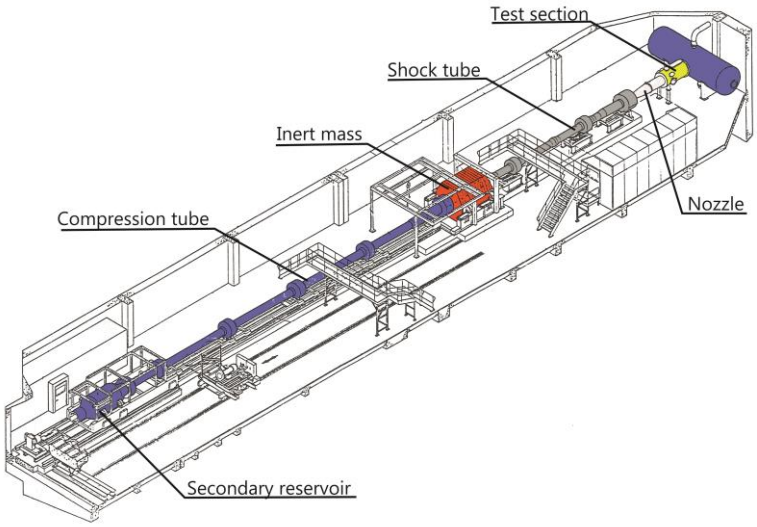

Fig 1. Schematic of HEG

In Fig 2 the typical temporal development of the reservoir pressure, free stream static pressure, free stream Pitot pressure and fuel equivalence ratio in the combustor of the SSFE scramjet engine is plotted. A nominal test time window of 3 ms is obtained.

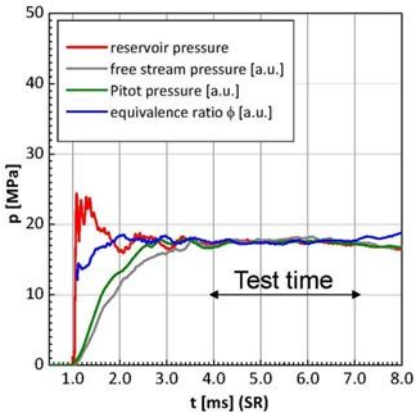

Fig 1. Typical temporal development of the nozzle reservoir pressure, free stream static pressure, free stream Pitot pressure and fuel equivalence ratio in the combustor of the SSFE engine; HEG operating condition XIII

Table 1. Nominal reservoir and free stream data for HEG operating condition XIII

p_0	[MPa]	18
h_0	[MJ/kg]	3.2
T_0	[K]	2700
p	[Pa]	2030
T	[K]	264
r	[g/m3]	27
u	[m/s]	2400
M	-	7.4

2.1. Model and Optical Setup

The model setup of the SSFE configuration in HEG, which is used to evaluate the thrust increment of the scramjet engine in free flight mode, is described in detail in [7,8,9]. It is schematically shown on the left part of Fig 2. The inlet of the model resides in the hypersonic nozzle (1). After the experiment in free flight mode, the model lands on the support structures (5) which are part of the catching system. These are installed on the HEG test section rail system (6). To adapt this system for the TSP measurements, the model setup is changed. The catching mechanism is modified to fix the model to the support structures and thus to the rail system (6). Further, the model can be tested at angles of attack. All other components of the free flight system are removed from the HEG test section.

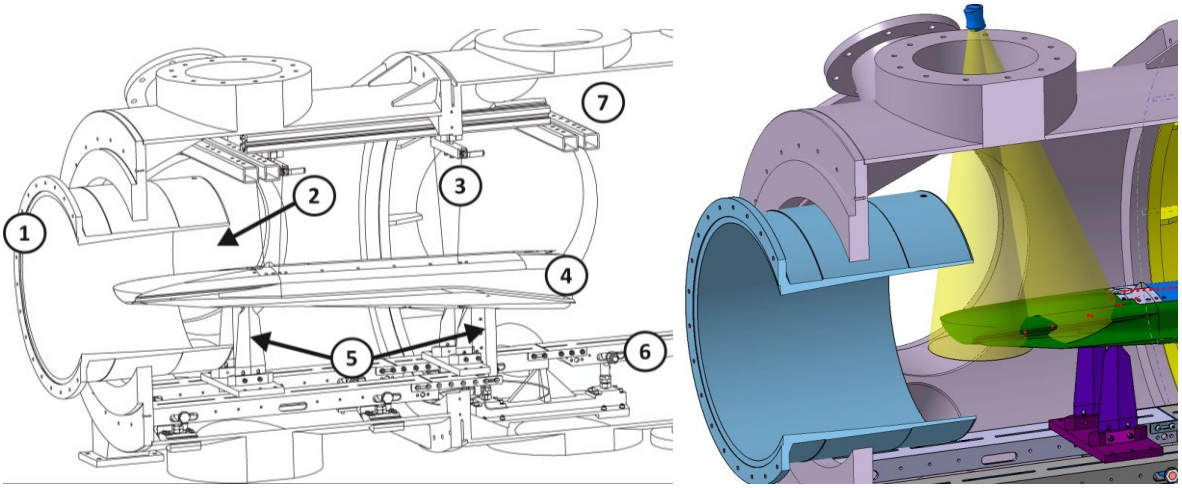

Fig 2. Schematic of the free flight SSFE model setup in the test section of HEG: (1) nozzle (2) intake (4) scramjet exhaust (5) catching system (6) rail system in the test section

The intake of the model is coated with a white insulating polyurethane base layer. This was sprayed and subsequently polished with sandpaper to the required surface roughness. The final thickness is measured at various positions and determined to be 100±7μm. The average surface roughness R_Z along the symmetry line of the intake at distances of x = 30 mm, x = 75 mm and x = 125 mm from the leading edge is 1.92 μm, 1.95 μm and 1.71 μm. The measurements have been obtained with a M2 perthometer manufactured by Mahr GmbH, Göttingen Germany (internal accuracy 0.5 μm).

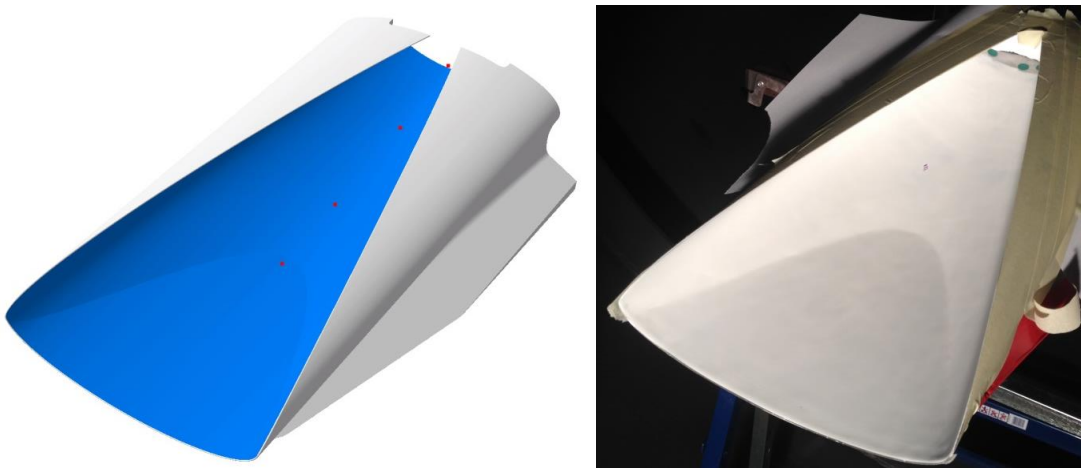

Fig 3. CAD drawing of the TSP coated area of the intake marked in blue (left); photograph of the model coated with the base layer in the test section of HEG (right)

The two images in Fig 3 show the coated area of the intake. The exact size of the area was extracted from the CAD geometry of the model and is A = 0.0945 m^2. In order to visualize the TSP layer which is coated onto the base layer, the camera is placed on top of the test section. The field of view is constraint since the window flange does not allow aligning the camera at large angles with respect to the model axis (right part of Fig 2). Two light emitting diodes (LEDs) are used to excite the TSP layer

on the intake. The LED light paths (very close to the camera field of view) illuminating the intake are also included in Fig 2. Two LEDs are used to obtain an optimum yield of the emitted light from the TSP layer. The two LEDs are shifted by an angle of approximately 20° to illuminate the complete surface of the intake. With this setting, the pixel count of the camera chip is 1000 (4096 is the maximum for the 12bit CCD chip of the camera) which is sufficient to obtain a good signal to noise ratio. The disadvantage of this setup is the region of high intensity, where the light paths of both LEDs overlap. However, due to the nature of the TSP data post processing, e.g., normalizing the recorded images by reference images (photometric TSP), the artefacts created by the overlapping region do not disturb the measurements. The density of the TSP layer is 1410 kg/m^3, based on the used mixing ratios of the elements of the TSP. Using the value of the coated area of the intake, the thickness of the TSP layer is determined to be 3±1μm. To calculate the TSP layer thickness, two assumptions are made. Firstly, the ethanol evaporates completely after the painting, and, secondly, the spraying is performed in such a way that the distribution of the color is homogenous.

2.2. Required Prerequisites for the Application of TSP in HEG

The underlying technique of TSP is that the color layer is excited by light with the appropriate wavelength in order to enforce fluorescence of the luminophores embedded in the TSP. The emitted fluorescence light is subsequently led to a detector (e.g. high speed camera). The excitation wavelength and the wavelength of the emitted light are separated by the Stokes shift. Due to this fact, the excitation and emission can be separated in wavelength by the use of a bandpass filter in front of the detector. The intensity of the excitation light is invers proportional to the temperature. A typical TSP setup is shown schematically in Fig 4 on the left. The application of TSP in a high enthalpy short duration facility like HEG requires that several prerequisites are fulfilled. The first requirement is to use a luminophore which exhibits small luminescence time, at least below τ≤1μs. The second is to use a thin TSP layer on the wind tunnel model surface and the third is that the TSP should not be influenced by the parasite light from the self-illumination of the flow. 4Methylumbelliferone (4MU) is chosen as luminophore for the present measurements. The luminophore has been applied in HEG in previous tests and has been proven to be a suitable candidate [10,11]. The luminescence time of 4MU is well below t_{res}≤1μs. The response time of the TSP layer is dependent on its thickness (see Fig 4).

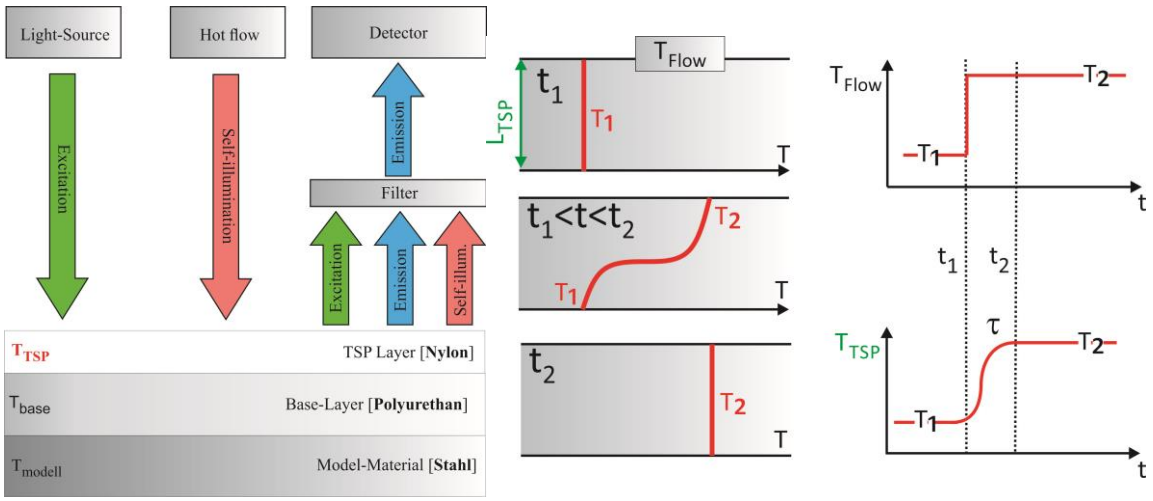

Fig 4. Schematic of the TSP technique (left), schematic of the temperature development in a TSP layer (right); the response time scales with the square of the layer thickness

The TSP layer is optically transparent and all excited molecules in the TSP layer will contribute to the excitation light signal. The temperature signal is, therefore, an averaged signal of the complete layer. The heat conduction through the TSP layer is a time dependent process and, therefore, an ideal step function will always be converted to a step response with a finite response time τ. To measure with TSP in high enthalpy short duration facilities, the TSP layer thickness should be smaller than 10μm, as discussed in [12]. This requirement is fulfilled in the present experiments as already pointed out above. The emission spectrum from a measurement in a region of stagnated flow for HEG condition XIII is shown in Fig 5 on the right. This spectral measurement of the flow self-illumination is a

mandatory step for the application of TSP in HEG to investigate the possibility of an additional excitation of the luminophore by the parasite light of flow self-illumination.

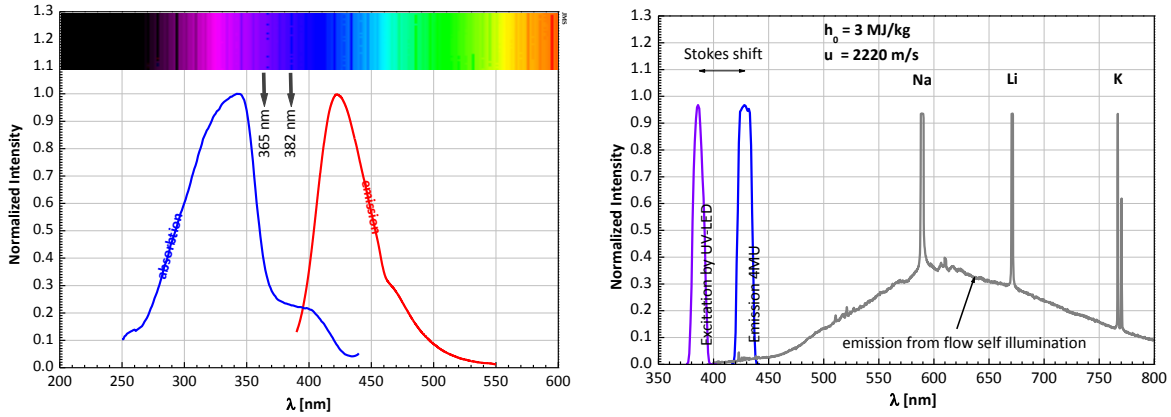

Fig 5. Absorption and emission spectra of the TSP luminophore used in the present experiments (left); filtered emission spectrum of the UV-LED used to excite the TSP luminophore and its corresponding emission spectrum in comparison to the spectral distribution of the emission from the flow self-illumination (right)

Fig 5 shows the absorption and emission distribution for 4MU on the left side. The present tests are performed by exciting 4MU with a UV LED emitting at 382 nm. As can be seen in Fig 5 on the left, this wavelength is not an optimal choice since the maximum of the absorption spectrum is located around 340 nm. Additionally, the quantum yield at this wavelength is only 0.25. However, LEDs with lower emission wavelengths (e.g. 365 nm) are only available with low and insufficient power. On the right side of Fig 5, the emission spectrum of 4MU is also shown, when exited at 382 nm. The maximum emission of 4MU is around 430 nm and thus sufficiently separated from the self-illumination wavelengths emitted from the test flow.

2.3. Data processing

The image data of the time dependent illumination of the TSP layer is recorded with a Phantom V1610 high speed camera with the "FAST" option installed. The image resolution is 806 x 432 px at a frame rate of f = 30 kHz. The exposure time of the chip is set to 25 μs. The images are converted to temperature applying a fit that has been calibrated for 4MU. More details on the calibration process and necessary steps to convert the bit count values of the camera to physical temperatures are given in [13]. The evaluation of the TSP data can subsequently follow that of thin-film gauges and other conventional sensors for heat-transfer measurements, as described in [1]. The base layer is treated as a uniform semi-infinite medium, and approximate solutions to the one-dimensional heat-conduction equation with appropriate boundary conditions are obtained. Thus, the surface heat flux can be computed from the time-dependent temperature profile as outlined in [14]:

$$q_s(t_n) = 2\sqrt{\frac{\rho c k}{\pi}} \sum_{i=1}^{n} \frac{T(t_i) - T(t_{i-1})}{\sqrt{t_n - t_i} + \sqrt{t_n - t_{i-1}}},$$

where $q_s(t_n)$ is the heat flux value at time t_n, $T(t_i)$ is the converted temperature at each pixel location, ρ is the density, c the heat capacity and k the heat conductivity of the base layer.

3. Results

The presented data results from two subsequent measurements. The complete intake is visualized and both experiments do not show significant differences. Therefore, the image data has been averaged to decrease to signal to noise ratio leading to an increased image quality.

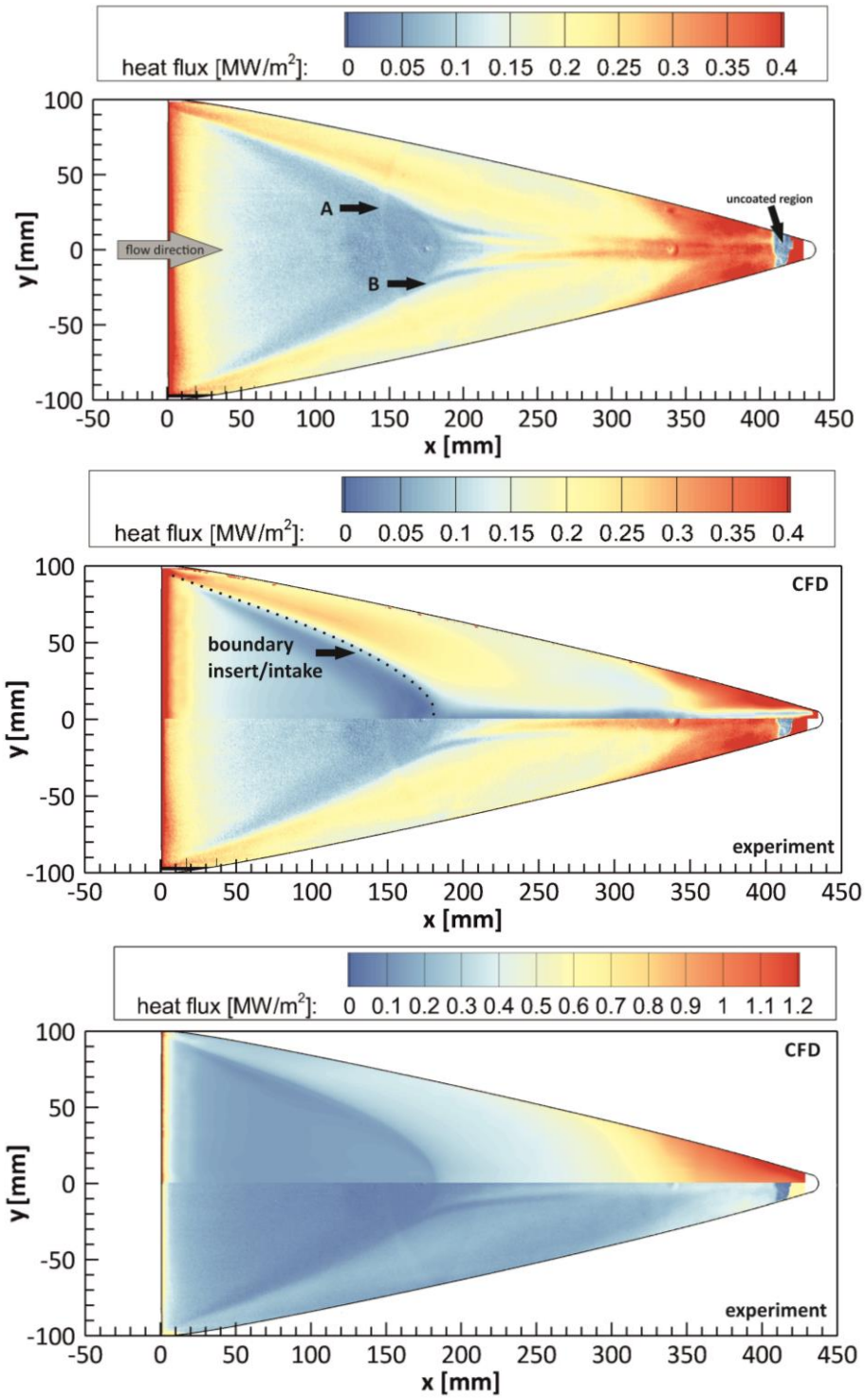

Fig 6. Experimental heat flux distribution measured on the intake with TSP (top); comparison between experiment and CFD assuming laminar flow (middle); comparison between experiment and CFD assuming turbulent flow (bottom)

The result is given in the top plot of Fig 6. The comparison to a numerical solution obtained with the DLR TAU code [15,16] assuming a fully laminar intake flow is given in the middle plot of Fig 6 and the comparison to a fully turbulent solution in the bottom plot of Fig 6. The inward turning intake was designed based on a modified Busemann flow field using a 3D stream tracing method [17]. It has an elliptical capture area with a ratio of major/minor axes of three and an overall contraction ratio of about nine. An elliptically shaped insert, indicated in the middle plot of Fig 6, was added in front of the actual intake surface. The wall surface heat flux increases downstream the insert due to the

compression of the flow. It should be pointed out, that the intake region slightly upstream of the combustor entrance (indicated in Fig 6 top) could neither be coated with a base layer nor with a TSP layer due to technical constraints. Therefore, the reduction of the heating at this point is an artefact and must be ignored for the data interpretation. As mentioned in the description of the experiment, two LEDs with an overlap region on the intake are used. As can be seen in the top plot of Fig 6, an artefact generated by this overlap region is visible after post processing of the data (point A). The direct comparison to the numerical laminar solution of the intake flow, as shown in the middle plot of Fig 6 and the comparison to the fully turbulent solution in the bottom plot reveals two distinct differences. The measured low heating level streak starting at point B and developing further downstream is not visible in the computed laminar and fully turbulent heat flux predictions. Comparing the laminar and fully turbulent numerical solution to the experimental data suggests that the boundary layer flow is in a transitional state. The fully turbulent solution significantly overestimates and the fully laminar solution underestimates the heating levels when compared to the measured data. In particular, the boundary layer heating in the symmetry plane along the downstream part of the intake is underestimated.

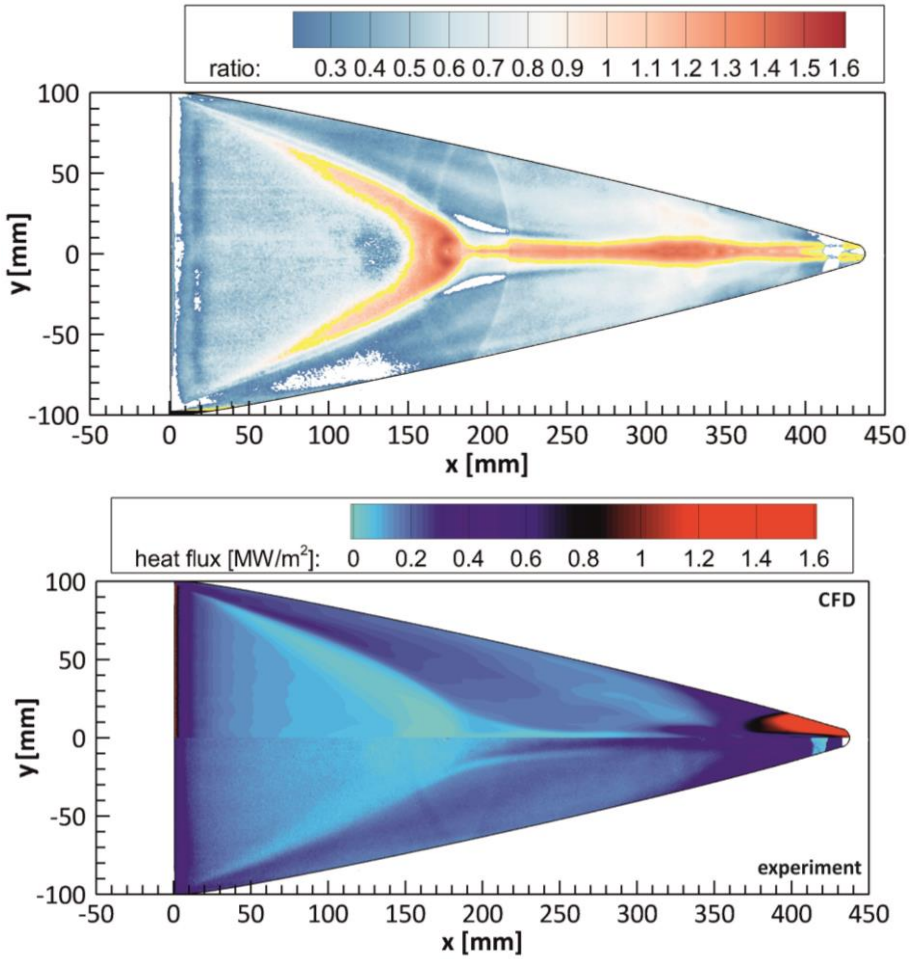

Fig 7. Ratio of the measured and computed laminar heat flux distribution; the yellow region highlights the ratio of 1 (top); heat flux distribution of the numerical transitional flow simulation (upper half) compared to the experimental data (lower half) (bottom)

Pursuing the goal to determine the boundary layer transition line from the TSP data, the ratio between the measured and computed laminar heat flux distribution is assessed (see top part of Fig 7). The distribution of this ratio reveals zones, where the laminar prediction underestimates the measured heat flux data. In particular, two distinct regions can be identified. The first horse shoe shaped region is located on the insert just upstream of the compression part of the intake. The second region is located along a narrow band on either side of the symmetry plane in the downstream part of the intake before the flow enters the combustor. Assuming that the identified

regions of enhanced wall heat flux are correlated with the laminar to turbulent boundary layer transition would indicate that the transition process is significantly more complex and different to a simple wedge shaped two dimensional intake ramp. The observed structure with a transitional region on the insert followed by a laminar region further downstream and the subsequent narrow band of transitional flow might be explained by high momentum laminar flow in the outer regions of the intake pushing the transitional flow towards the symmetry plane, ultimately forming the identified narrow band of transitional flow in the downstream part. However, in order to verify this hypothesis additional analysis would be required. Another explanation of the elevated heat flux level on the insert could be the presence of a separated flow region detected in the laminar solution which might not occur in the experiment.

In a first attempt to compute the transitional flow on the intake, the boundary of the second region with elevated heat flux was used as transition line and a shock-corrected Reynolds stress turbulence model [18] was applied. More details on the numerical scheme used for the simulation are given in [19,20]. The numerically predicted wall heat flux is compared to the measured data in Fig 7. From the two dimensional data given in Fig 7, one dimensional cuts are extracted and presented in Fig 8. Here, cuts in streamwise and cross direction are given.

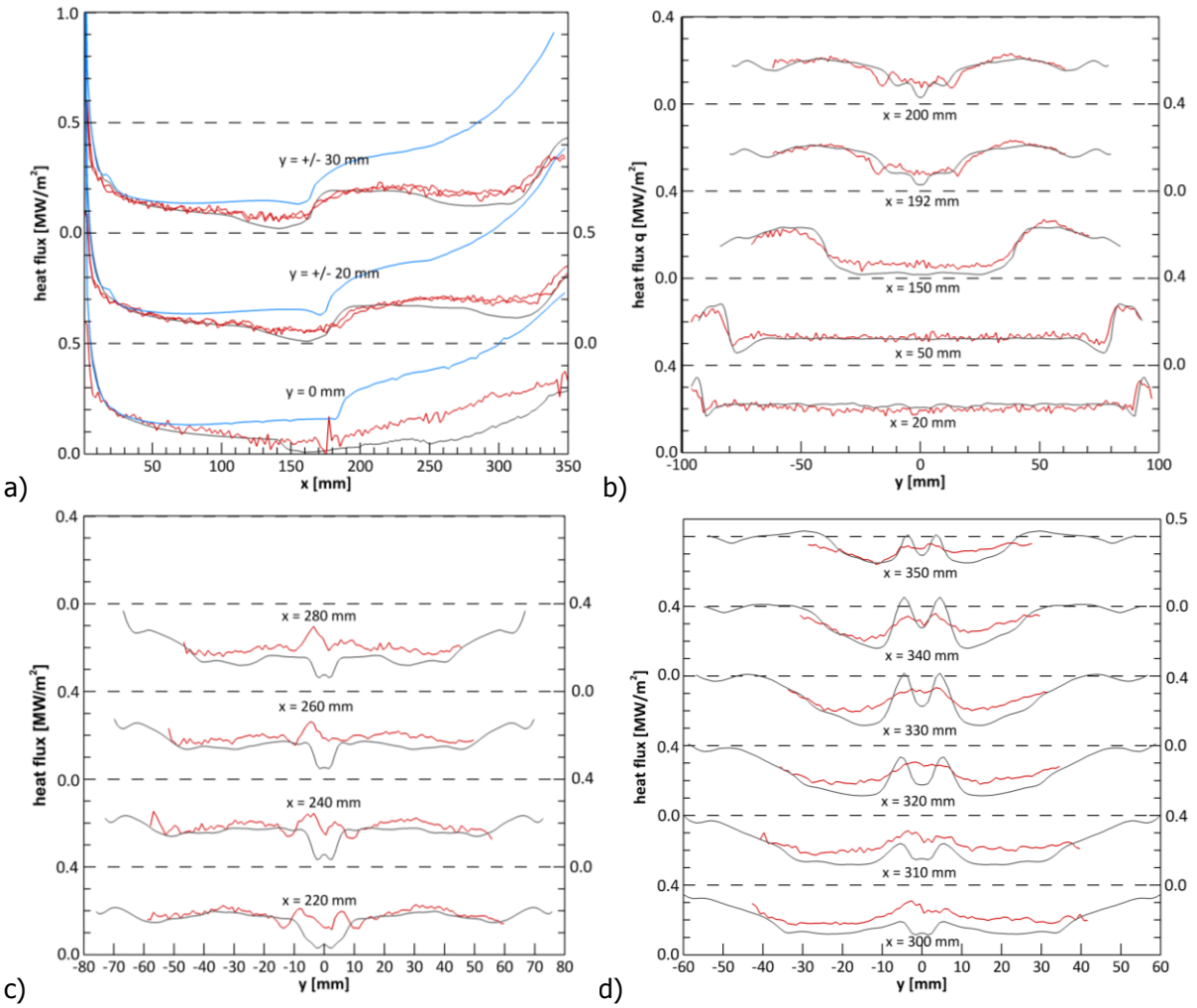

Fig 8. Heat flux distributions along various streamwise cuts (a) and cuts in cross to direction (b) – (d); numerical transitional data (gray lines), numerical fully turbulent data (blue lines) and experimental data (red lines)

Along the streamwise cuts the difference between experiment and numerical simulation on the upstream part of the insert region is within a few per cent (see Fig 8 a). Deviations are identified along the symmetry plane for x > 150 mm (Fig 8 a). Here, the numerical scheme under predicts the heating on the intake up to a factor of 4. The comparison for the extracted data in cross direction given in Fig 8 b) shows very good agreement on the intake insert for x < 150 mm, where the flow is

modelled as laminar. In the region of the horse shoe region (x ≈ 150 mm), the computed data underestimates the measured values. The extracted data in Fig 8 c) and Fig 8 d) show the region downstream of the junction between the insert and the compression part of the intake and upstream of the combustor entrance. Since the flow properties at the combustor entrance strongly depend on the boundary layer history along the intake, the comparison of the surface heat flux directly in front of the combustor entrance is of particular interest. It can be observed that the difference between numerical and experimental heat flux data is decreased when approaching the combustor entrance. While the difference at x = 300 mm is around a factor of four in the vicinity of the symmetry line, the mean difference at x = 350 mm is significantly reduced. The numerical data exhibits two distinct maxima of surface heating away from the symmetry plane [20], which are not visible in the experimental data. The comparison between the computed transitional and fully turbulent wall heat flux distributions with the measured data along the streamwise cuts in Fig 8 a) shows that the transitional flow model significantly improves the comparison between CFD and experiment.

4. Summary and Conclusions

Heat flux measurements on the intake of the LAPCAT II small scale flight experiment (SSFE) configuration utilizing fast response temperature sensitive were conducted in the High Enthalpy Shock Tunnel Göttingen, HEG. Based on a combined experimental / numerical data evaluation procedure, an estimate of the laminar to turbulent boundary layer transition line could be determined. A hypothesis explaining the complex observed transition behaviour on the three-dimensional intake flow was given. A first attempt to model the transitional intake flow using a transition line extracted from the downstream region of elevated heat flux revealed significant improvements compared to fully turbulent flow predictions. The remaining differences between computed and measured wall heat flux might be caused by neglecting the first horse shoe shaped region of elevated measured heat flux compared to the laminar flow predictions. In order to study the influence of both selected regions of potentially transitional flow step by step, the impact of the first region on the heat flux predictions on the intake will be the objective of a future study.

References

1. Schultz DL, Jones TV, Heat transfer measurements in short-duration hypersonic facilities, AGARD-AG-165, 1973
2. Steelant, J., Sustained Hypersonic Flight in Europe: Technology Drivers for LAPCAT II, AIAA 2009-7240, 16th AIAA/DLR/DGLR International Space Planes and Hypersonic System Technologies Conference. Bremen, Germany:, 2009
3. Deutsches Zentrum für Luft - und Raumfahrt (DLR). (2018). The High Enthalpy Shock Tunnel Göttingen of the German Aerospace Center (DLR). Journal of large-scale research facilities, 4, A133. http://dx.doi.org/10.17815/jlsrf-4-168
4. Hannemann, K., Martinez Schramm, J., High Enthalpy, High Pressure Short Duration Testing of Hypersonic Flows, In: Springer Handbook of Experimental Fluid Mechanics, pp. 1081 – 1125, Springer Berlin Heidelberg, Eds.: Tropea, C., Foss, J., Yarin, A., 2007
5. Hannemann, K., Martinez Schramm, J., Karl, S., Recent extensions to the High Enthalpy Shock Tunnel Göttingen (HEG), Proceedings of the 2nd International ARA Days "Ten Years after ARD", Arcachon, France, 21-23 October, 2008
6. Stalker, R.J., A Study of the Free-Piston Shock Tunnel, AIAA Journal, Vol. 5, No. 12, 1967
7. Hannemann, K., Karl, S., Martinez Schramm, J., Steelant, J., Methodology of a Combined Ground Based Testing and Numerical Modelling Analysis of Supersonic Combustion Flow Paths, Shock Waves, Springer, Volume 20, Number 5, pp. 353-366, 2010
8. Hannemann, K., Martinez Schramm, J., Laurence, S., Karl, S., Langener, T., Steelant, J., Experimental and Numerical Analysis of the small Scale LAPCAT II Scramjet Flow Path

in High Enthalpy Shock Tunnel Conditions, SP2014-2969350, Proceedings Space Propulsion 2014, Cologne, Germany, 19-22 May, 2014

9. Hannemann, K., Martinez Schramm, J., Laurence, S., Karl, S., Shock Tunnel Free Flight Force Measurements Using a Complex Model Configuration, Proceedings 8th European Symposium on Aerothermodynamics for Space Vehicles, Lisbon, Portugal, March 2 - 6, 2015
10. Martinez Schramm, J., Edzards, F. and Hannemann, K, Development of Ultra-fast Temperature Sensitive Paints for Hypersonic High Speed Flows, 21st AIAA International Space Planes and Hypersonics Technologies Conference, International Space Planes and Hypersonic Systems and Technologies Conferences, (AIAA 2017-2211) https://doi.org/10.2514/6.2017-2211
11. Stuart J. Laurence, Hiroshi Ozawa, Jan Martinez Schramm, and Klaus Hannemann. "Time-resolved temperature sensitive paint measurements on a hypersonic intake ramp", 22nd AIAA International Space Planes and Hypersonics Systems and Technologies Conference, AIAA SPACE Forum, (AIAA 2018-5383), https://doi.org/10.2514/6.2018-5383
12. Martinez Schramm, J., Hannemann, K., Ozawa, H., Beck, W., Klein C., Development of Temperature Sensitive Paints for the High Enthalpy Shock Tunnel Göttingen, HEG. 8th European Symposium on Aerothermodynamics for Space Vehicles, Lissabon, Portugal, 2015
13. Martinez Schramm, J., Edzards, F. Hannemann, K., Calibration of Fast-Response Temperature Sensitive Paints for their Application in Hypersonic High Enthalpy Flows, New Results in Numerical and Experimental Fluid Mechanics XI, Notes on Numerical Fluid Mechanics and Multidisciplinary Design, Editors: Andreas Dillmann, Gerd Heller, Ewald Krämer, Rolf Radespiel, Claus Wagner, Springer, 2017
14. Cook, W.J., Felderman, E.J., Reduction of Data from Thin-Film Heat Transfer Gage: A Concise Numerical Technique, AIAA J 4(3):561-562, 1966
15. Schwamborn, D., Gerhold, T., and Heinrich, R., The DLR Tau-Code: Recent Applications in Research and Industry, Proceedings of the European Conference on Computational Fluid Dynamics ECCOMAS, edited by Wesseling, P., Onate, E., and Periaux, J.,TU Delft, The Netherlands, 2006
16. Gerhold, T., Overview of the Hybrid RANS Code TAU, in: MEGAFLOW-Numerical Flow Simulation for Aircraft Design, edited by Kroll, N., and Fassbender, J. K.,Vol. 89, Notes on Numerical Fluid Mechanics and Multidisciplinary Design, Springer, Berlin, pp. 81–92,2005
17. Karl, S. and Steelant, J.: Crossflow Phenomena in Streamline-Traced Hypersonic Intakes, Journal of Propulsion and Power, Vol. 34, No. 2, pp. 449-459, 2018
18. Karl, S., Hickey, J. P. and Lacombe, F.: Reynolds Stress Models for Shock – Turbulence Interaction, 31st International Symposium on Shock Waves, 09.-14.Juli 2017, Nagoya, Japan
19. Karl, S.: Numerical Investigation of a Generic Scramjet Configuration, Ph.D. Dissertation, Faculty of Mech. Eng., Technical University Dresden, 2011, [available online] URL: http://nbnresolving.de/urn:nbn:de:bsz:14-qucosa-68695 [cited Jan. 2017]
20. Karl, S., Martinez Schramm, J., Hannemann, K., Post-Test Analysis of the LAPCAT-II Subscale Scramjet, HiSST: International Conference on High-Speed Vehicle Science Technology, Paper 2018-0846, Moscow, Nov. 26-29, 2018

